

Four harmonic analysis and energy metering algorithms based on a new cosine window function

Shuangyong Zhuang^{1,2}, Wei Zhao¹, Qing Wang³, Songling Huang¹

¹Department of Electrical Engineering, Tsinghua University, Beijing, People's Republic of China

²Department of Metrology and Testing, Beijing Aerospace Control Center, Beijing, People's Republic of China

³Department of Engineering, Durham University, Durham, UK

E-mail: zhaowei@mail.tsinghua.edu.cn

Published in *The Journal of Engineering*; Received on 17th November 2017; Accepted on 24th November 2017

Abstract: In order to further improve the calculation accuracy of the windowed fast Fourier transform (FFT) interpolation algorithm, this study proposes a four-order Hanning self-multiplication window, and based on this new window function, four kinds of windowed FFT interpolation algorithms for harmonic analysis have been derived, include single-spectrum-line interpolation, double-spectrum-line interpolation, triple-spectrum-line interpolation and four-spectrum-line interpolation. Using these four harmonic analysis algorithms, the amplitude, phase and frequency of the fundamental and harmonic in the measured voltage and current signal can be obtained, and then the fundamental and harmonic energy can be calculated accurately by using the energy metering equation. The simulation results show that the window function has better main lobe and side lobe performance, which can effectively suppress the influence of spectrum leakage and fence effect, so based on this window function, the four harmonic analysis and energy metering algorithms can inhibit the effect of fundamental frequency fluctuation, and with the number of spectrum lines increasing, the computing accuracy of the algorithm is improved.

1 Introduction

More and more non-linear dynamic power loads are being put into use in power supply systems, like electrified railways, electric arc furnaces etc., which produce a lot of power harmonics, resulting in the supply of current and voltage waveform distortion. The existence of these disturbances not only lead to the deterioration of the quality of the power supply, endangering the safe and stable operation of the power supply system, but also affect the accuracy of energy metering [1].

In order to accurately measure fundamental and harmonic energy, we should first accurately extract the amplitude, frequency [2, 3] and phase parameters [4–6] of the fundamental and harmonics in the grid voltage and current signals. The common method is to apply the window function to the measured signal, Fourier transform [7], interpolation correction [8, 9] and other operations. In other words, before applying FFT to the measured signal, we apply the appropriate window function to suppress the spectral leakage [10] caused by asynchronous sampling and non-periodic cut-off. Then, the windowed signal is transformed to the frequency domain by FFT and the discrete spectrum is obtained. Finally, we use one kind of interpolation correction algorithm to compensate the error caused by the fence effect.

The so-called appropriate window function [11, 12] should have the characteristics that the main-lobe width is narrow, the side-lobe peak level is low and the side-lobe roll-off rate is faster. Up to now, some scholars have designed a variety of basic window functions, mainly include rectangular window, Hanning window [13], Blackman window [14], Blackman–Harris window [15], Rife–Vincent window [10], Nuttall window [16], Kaiser window [17] and various combinations of cosine windows and so on. In recent years, some scholars have proposed a variety of improved window functions on the basis

of the existing window function. As shown in [18], the Hanning self-convolution window function is proposed. In [19], a self-multiplication window function is proposed. Although the main-lobe of the self-multiplication window function becomes wide, the frequency resolution decreases, and the amount of calculation increases with the increase of the self-multiplication order.

The interpolation correction is to use a single, two or more spectrum lines [20] around the actual measured frequency point to calculate the frequency and amplitude correction coefficient, and then the actual measured frequency point spectrum amplitude, phase and frequency parameters are calculated by interpolation. Commonly used interpolation algorithms include the single-spectrum-line interpolation (SSLI), double-spectrum-line interpolation (DSLII), triple-spectrum-line interpolation (TSLI) [21] and four-spectrum-line interpolation (FSLI). In the four kinds of interpolation correction algorithms, the SSLI algorithm is more complex and susceptible to spectrum leakage. The DSLII algorithm is not sufficient to use the spectrum leakage near the measured frequency point, and the TSLI algorithm does not fully consider the full information of the symmetry spectrum of the measured frequency point. The FSLI algorithm has the highest accuracy, but the calculation is also the largest.

In order to further improve the computational accuracy of the windowed FFT interpolation algorithm, this paper tries to design a novel five-item cosine combination window function with a narrow main-lobe width, a lower side-lobe peak level and a faster side-lobe roll-off rate based on the widely used Hanning window function. Then, based on the new window function, the four kinds of harmonic analysis and energy metering algorithms of SSLI, DSLII, TSLI and FSLI are derived separately, which can greatly improve the computing accuracy of the fundamental and harmonic energy metering.

2 Design of new type five-term cosine window

The discrete time-domain expression of the basic Hanning window function is shown in the following equation:

$$\text{whan}(n) = \frac{1}{2} - \frac{1}{2} \cdot \cos\left(2\pi \cdot \frac{n}{N}\right), \quad n = 0, 1, \dots, N-1 \quad (1)$$

where N is the width or length of the Hanning window.

The discrete expression of the four-order Hanning self-multiplication window (FHSMW) function is

$$\begin{aligned} w(n) = [\text{whan}(n)]^4 = & \frac{35}{128} - \frac{7}{16} \cdot \cos\left(2\pi \cdot \frac{n}{N}\right) \\ & + \frac{7}{32} \cdot \cos\left(4\pi \cdot \frac{n}{N}\right) - \frac{1}{16} \cdot \cos\left(6\pi \cdot \frac{n}{N}\right) \\ & + \frac{1}{128} \cdot \cos\left(8\pi \cdot \frac{n}{N}\right), \quad n = 0, 1, \dots, N-1 \end{aligned} \quad (2)$$

It can be seen from the discrete expression of the FHSMW function that its coefficients satisfy the conditions as shown in the following equation:

$$\sum_{m=0}^{M-1} \alpha_m = 1, \quad \sum_{m=0}^{M-1} (-1)^m \alpha_m = 0 \quad (3)$$

where α_m and M are coefficient values and the number of coefficients of the window function, respectively.

Therefore, this FHSMW function belongs to a new type of four-term cosine window function, called FHSMW, and its frequency-domain expression is obtained using the discrete Fourier transform (DFT), which is given as

$$\begin{aligned} W(\omega) = & \frac{35}{128} W_R(\omega) - \frac{7}{32} \left[W_R\left(\omega - \frac{2\pi}{N}\right) + W_R\left(\omega + \frac{2\pi}{N}\right) \right] \\ & + \frac{7}{64} \left[W_R\left(\omega - \frac{4\pi}{N}\right) + W_R\left(\omega + \frac{4\pi}{N}\right) \right] \\ & - \frac{1}{32} \left[W_R\left(\omega - \frac{6\pi}{N}\right) + W_R\left(\omega + \frac{6\pi}{N}\right) \right] \\ & + \frac{1}{256} \left[W_R\left(\omega - \frac{8\pi}{N}\right) + W_R\left(\omega + \frac{8\pi}{N}\right) \right] \end{aligned} \quad (4)$$

where ω is the angular frequency, and $W_R(\omega)$ is the DFT of a rectangular window, which can be written as

$$W_R(\omega) = \frac{\sin(\omega N/2)}{\sin(\omega/2)} e^{-j\omega(N-1)/2} \quad (5)$$

The main-lobe width of the window function is defined as the distance between the nearest two zero-crossing points on both sides of the frequency-domain origin. So, when $|W(\omega)| = 0$, the frequency-domain expression should meet the condition

$$\begin{cases} \frac{N}{2} \left(\omega \pm \frac{2\pi}{N} m \right) = d\pi \\ \frac{1}{2} \left(\omega \pm \frac{2\pi}{N} m \right) \neq d\pi \end{cases} \quad m = 0, 1, 2, 3, 4; \quad (6)$$

$$d = 0, \pm 1, \dots, \pm \infty$$

When $d = \pm 1$ and $m = 4$, the main-lobe width of FHSMW is $Bw = (20\pi/N)$.

The amplitude-frequency characteristics of FHSMW are shown in Fig. 1.

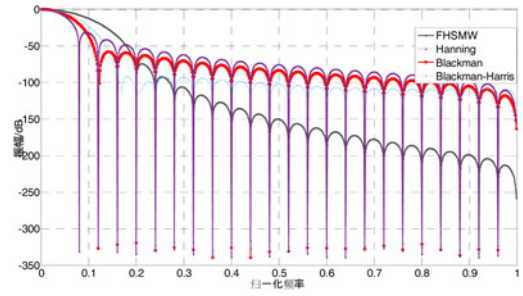


Fig. 1 Amplitude-frequency characteristics of four window

Compared with the Hanning window, Blackman window and Blackman-Harris window, the FHSMW has a wider main-lobe width, but the side-lobe performance has been improved greatly, the peak side-lobe level is -74.6 dB and the side-lobe roll-off rate is 75 dB/octave.

3 Principle and derivation of four kinds of harmonic analysis and energy metering algorithms

Assuming that a time-domain signal with multi-harmonic components is sampled at a sampling rate f_s , the discrete sequence is obtained as

$$x(n) = \sum_{m=1}^M A_m \cdot \sin\left(2\pi \frac{f_0}{f_s} mn + \theta_m\right) \quad (7)$$

where M is the number of fundamental and harmonic components, m is the order of the harmonic, f_0 is the fundamental frequency, and A_m and θ_m are the amplitude and phase of the m th harmonic, respectively. Equation (7) is expressed in Euler formula as

$$x(n) = \sum_{m=1}^M \frac{A_m}{2j} \cdot (e^{j\theta_m} e^{j2\pi(f_0/f_s)mn} - e^{-j\theta_m} e^{-j2\pi(f_0/f_s)mn}) \quad (8)$$

The discrete sequence of the FHSMW is $w(n)$ and its spectrum is $W(2\pi f/f_s)$, so the frequency-domain expression of the windowed $x(n)$ is obtained by applying DFT, as shown in the following equation:

$$\begin{aligned} X(f) = & \sum_{n=-\infty}^{+\infty} x(n) \cdot w(n) e^{-j2\pi(f/f_s)n} \\ = & \sum_{m=1}^M \frac{A_m}{2j} \left[e^{j\theta_m} W\left(\frac{2\pi(f - mf_0)}{f_s}\right) - e^{-j\theta_m} W\left(\frac{2\pi(f + mf_0)}{f_s}\right) \right] \end{aligned} \quad (9)$$

Due to the negative frequency, $-mf_0$ is a calculated result and has no effect on the actual spectrum, which can be neglected, so the final frequency-domain expression of the windowed $x(n)$ is shown as

$$X(f) = \sum_{m=1}^M \frac{A_m}{2j} \left[e^{j\theta_m} W\left(\frac{2\pi(f - mf_0)}{f_s}\right) \right] \quad (10)$$

Through discrete sampling, the expression of the DFT is obtained as

$$X(k \cdot \Delta f) = \sum_{m=1}^M \frac{A_m}{2j} \left[e^{j\theta_m} W\left(\frac{2\pi(k \cdot \Delta f - mf_0)}{f_s}\right) \right] \quad (11)$$

where $\Delta f = f_s/N$ is the frequency resolution, k is the k th spectrum line and m is the m th harmonic order.

3.1 Derivation of SSLI harmonic analysis algorithm

In order to simplify the derivation process, it is assumed that the signal contains only fundamental component, and then the derivation of other harmonic components is given as

$$X(k \cdot \Delta f) = \frac{A}{2j} \left[e^{j\theta} W \left(\frac{2\pi(k \cdot \Delta f - k_0 \cdot \Delta f)}{f_s} \right) \right] \quad (12)$$

Due to spectral leakage and fence effect, the actual harmonic frequency $f_0 = k_0 \Delta f$ is generally difficult to fall on the discrete spectrum line, that is, to say, k_0 is generally not an integer. Assuming that the two spectral lines on the left and right sides of the measured actual frequency point are the k_1 th and the k_2 th, respectively, which correspond to the maximum and secondary spectrum line on both sides of the actual harmonic frequency point, the spectrum is shown in Fig. 2, where k_0 is the actual spectrum line, and k_1 and k_2 are the biggest two spectrum lines around k_0 . When the actual frequency of the power system is bigger than 50 Hz, the selected two spectrum lines and actual spectrum line are shown in Fig. 2a, else if the actual fundamental frequency of the power system is <50 Hz, then the spectrum line distribution is shown in Fig. 2b.

Here, a parameter $\alpha = k_0 - k_1$ ($\alpha \in [0, 1]$) is introduced, and the amplitude of spectrum lines k_1 and k_2 are $y_1 = |X(k_1 \cdot \Delta f)|$ and $y_2 = |X(k_2 \cdot \Delta f)|$, respectively. The ratio $\beta = y_2/y_1$ of the two spectrum line amplitude is obtain as

$$\beta = \frac{|W[2\pi(1 - \alpha)/N]|}{|W[2\pi(-\alpha)/N]|} = f(\alpha) \quad (13)$$

According to the polynomial fitting, the inverse function $\alpha = f^{-1}(\beta)$ is obtained, that is, the frequency correction coefficient is

$$\begin{aligned} \alpha = & -4.46411652 + 8.67685357 \cdot \beta - 7.67410367 \cdot \beta^2 \\ & + 5.68058956 \cdot \beta^3 - 3.21181305 \cdot \beta^4 + 1.26158143 \cdot \beta^5 \\ & - 0.30186941 \cdot \beta^6 + 0.03287809 \cdot \beta^7 \end{aligned} \quad (14)$$

The amplitude correction formula is more complex and needs to be further optimised. So, let $\gamma = k_0 - k_i$, if $0 \leq \alpha \leq 0.5$, that is, the actual fundamental frequency is bigger than 50 Hz, as shown in Fig. 2a, then $k_i = k_1$, so $\gamma = \alpha$, else $k_i = k_2$, as shown in Fig. 2b, then $\gamma = -(1 - \alpha)$. So, the larger amplitude of the two spectrum

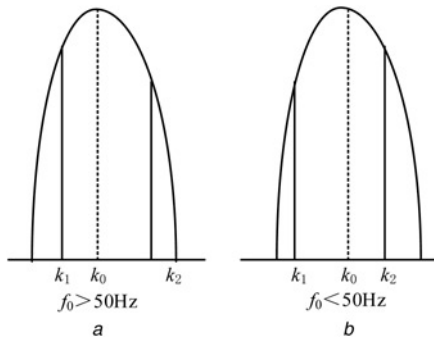


Fig. 2 Distribution of double spectrum lines

lines can be expressed as

$$y_i = \frac{1}{2} \cdot A \cdot |W[2\pi(-\gamma)/N]|$$

After transformation, the amplitude correction formula is given as

$$A = \frac{2y_i}{|W[2\pi(-\gamma)/N]|} \quad (15)$$

where A is the amplitude of the fundamental, which can be calculated accurately by the interpolation algorithm derived later. Let $g(\gamma) = 2N/|W[2\pi(-\gamma)/N]|$. According to the polynomial fitting, the amplitude correction coefficient is given as

$$\begin{aligned} g(\gamma) = & 7.31428569 + 1.6188229 \cdot \gamma^2 \\ & + 0.19212372 \cdot \gamma^4 + 0.01689194 \cdot \gamma^6 \end{aligned} \quad (16)$$

So, the amplitude interpolation formula of SSLI algorithm is

$$A = y_i \cdot g(\gamma)/N \quad (17)$$

The phase interpolation formula is

$$\theta = \arg [X(k_i \Delta f)] + \frac{\pi}{2} - \pi \cdot \alpha \quad (18)$$

Also, the frequency interpolation formula is

$$f_0 = k_0 \Delta f = (k_i - 1 + \alpha) \cdot f_s/N \quad (19)$$

where if the actual frequency of the power system is larger than 50 Hz, then i equals 1, else i equals 2.

3.2 Derivation of DSLI harmonic analysis algorithm

The derivation of the DSLI algorithm is shown in Fig. 2. Assuming that the parameter $\alpha = k_0 - k_1 - 0.5$ ($\alpha \in [-0.5, 0.5]$), and let the parameter of the amplitude ratio $\beta = (y_2 - y_1)/(y_2 + y_1)$, we obtain the following equation:

$$\begin{aligned} \beta = & \frac{|W[2\pi(-\alpha + 0.5)/N]| - |W[2\pi(-\alpha - 0.5)/N]|}{|W[2\pi(-\alpha + 0.5)/N]| + |W[2\pi(-\alpha - 0.5)/N]|} \\ = & f(\alpha) \end{aligned} \quad (20)$$

According to the polynomial fitting, the frequency correction coefficient is

$$\alpha = 4.5 \cdot \beta \quad (21)$$

From the equation

$$\begin{aligned} y_1 + y_2 = & \frac{1}{2} \cdot A \cdot \{ |W[2\pi(-\alpha - 0.5)/N]| \\ & + |W[2\pi(-\alpha + 0.5)/N]| \} \end{aligned} \quad (22)$$

The amplitude correction formula of A is expressed as

$$A = \frac{2(y_1 + y_2)}{|W[2\pi(-\alpha - 0.5)/N]| + |W[2\pi(-\alpha + 0.5)/N]|} \quad (23)$$

Let

$$g(\alpha) = \frac{2 \cdot N}{|W[2\pi(-\alpha - 0.5)/N]| + |W[2\pi(-\alpha + 0.5)/N]|}$$

According to the polynomial fitting, the amplitude correction coefficient is given as

$$g(\alpha) = 3.86563158 + 0.77058541 \cdot \alpha^2 + 0.08183360 \cdot \alpha^4 + 0.00636824 \cdot \alpha^6 \quad (24)$$

So, the amplitude correction formula of the DSLI algorithm is

$$A = (y_1 + y_2) \cdot g(\alpha)/N \quad (25)$$

The phase correction formula is

$$\theta = \arg [X(k_1 \cdot \Delta f)] + \frac{\pi}{2} - \pi \cdot (\alpha - (-1)^i \cdot 0.5) \quad (26)$$

Also, the frequency correction formula is

$$f_0 = k_0 \cdot \Delta f = (k_i - 1 + 0.5 + \alpha) \cdot f_s/N \quad (27)$$

In which, if the actual frequency of the power system is larger than 50 Hz, then i equal 1, else i equal to 2.

The amplitude of the actual frequency point is obtained by weighting the maximum spectral amplitude and the next maximum spectral amplitude on both sides of the peak point. Therefore, the algorithm is called the DSLI algorithm.

3.3 Derivation of TSLI harmonic analysis algorithm

For this kind of algorithm, three spectrum lines are selected. One of the lines is the maximum spectrum k_1 around the actual frequency point k_0 , and the other two spectrum lines are k_2 and k_3 , as shown in Fig. 3.

When the actual fundamental frequency of the power system is bigger than 50 Hz, the distribution of the spectrum lines is shown in Fig. 3a, else if the actual fundamental frequency of the power system is <50 Hz, then the distribution of the spectrum lines is shown in Fig. 3b.

Assuming that the parameter $\alpha = k_0 - k_1$, for $k_2 = k_1 - 1 \leq k_1 \leq k_3 = k_1 + 1$, so $\alpha \in [-0.5, 0.5]$, and the corresponding amplitudes are $y_1 = |X(k_2 \cdot \Delta f)|$, $y_2 = |X(k_1 \cdot \Delta f)|$ and $y_3 = |X(k_3 \cdot \Delta f)|$, respectively. Let the parameter of the amplitude ratio $\beta = (y_3 - y_1)/y_2$, the following equation is obtained:

$$\beta = \frac{|W[2\pi(1 - \alpha)/N]| - |W[2\pi(-1 - \alpha)/N]|}{|W[2\pi(-\alpha)/N]|} = f(\alpha) \quad (28)$$

According to the polynomial fitting, the frequency correction coefficient is given as

$$\alpha = 1.38888888 \cdot \beta - 0.10716678 \cdot \beta^3 + 0.01652129 \cdot \beta^5 - 0.00300526 \cdot \beta^7 \quad (29)$$

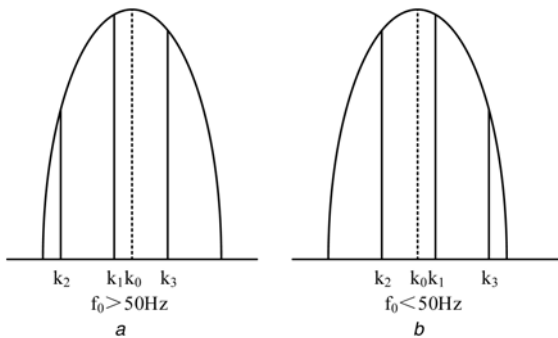


Fig. 3 Distribution of triple spectrum lines

For

$$y_1 + 2y_2 + y_3 = \frac{1}{2} \cdot A \cdot \{|W[2\pi(-1 - \alpha)/N]| + 2 \cdot |W[2\pi(-\alpha)/N]| + |W[2\pi(1 - \alpha)/N]|\},$$

the amplitude correction formula is obtained as

$$A = \frac{2(y_1 + 2y_2 + y_3)}{|W[2\pi(-1 - \alpha)/N]| + 2 \cdot |W[2\pi(-\alpha)/N]| + |W[2\pi(1 - \alpha)/N]|} \quad (30)$$

Let

$$g(\alpha) = \frac{2 \cdot N}{|W[2\pi(-1 - \alpha)/N]| + 2 \cdot |W[2\pi(-\alpha)/N]| + |W[2\pi(1 - \alpha)/N]|}$$

and according to the polynomial fitting, the amplitude correction coefficient is

$$g(\alpha) = 2.03174603 + 0.36840261 \cdot \alpha^2 + 0.03539348 \cdot \alpha^4 + 0.00246968 \cdot \alpha^6 \quad (31)$$

So, the amplitude correction formula of the TSLI algorithm is

$$A = (y_1 + 2y_2 + y_3) \cdot g(\alpha)/N \quad (32)$$

The phase correction formula is

$$\theta = \arg [X(k_1 \cdot \Delta f)] + \frac{\pi}{2} - \pi \cdot \alpha \quad (33)$$

Also, the frequency correction formula is

$$f_0 = k_0 \cdot \Delta f = (k_1 - 1 + \alpha) \cdot f_s/N \quad (34)$$

3.4 Derivation of FSLI harmonic analysis algorithm

For this algorithm derivation, the nearest four spectrum lines k_1 , k_2 , k_3 and k_4 around the actual frequency point k_0 are used, and the corresponding amplitudes are $y_1 = |X(k_1 \cdot \Delta f)|$, $y_2 = |X(k_2 \cdot \Delta f)|$, $y_3 = |X(k_3 \cdot \Delta f)|$ and $y_4 = |X(k_4 \cdot \Delta f)|$, respectively. The distribution of the spectrum lines is shown in Fig. 4.

When the actual fundamental frequency of the power system is bigger than 50 Hz, the distribution of the spectrum lines is as shown in Fig. 4a, else if the actual fundamental frequency of the power system is <50 Hz, then the illustration is as shown in Fig. 4b.

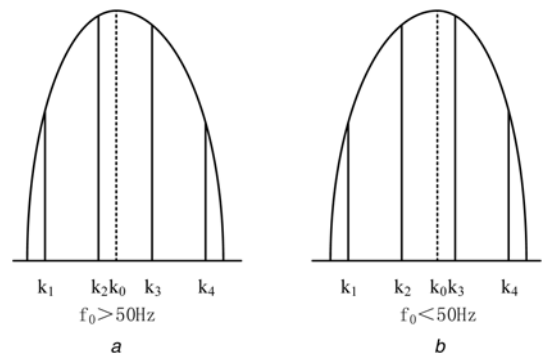


Fig. 4 Distribution of four spectrum lines

Let the parameter $\alpha = k_0 - k_2 - 0.5$ ($\alpha \in [-0.5, 0.5]$), the amplitude ratio is $\beta = ((2y_3 + y_4) - (2y_2 + y_1))/(y_1 + 2y_2 + 2y_3 + y_4)$. In order to simplify the formula, let $R = 2y_3 + y_4 = 2 \cdot |W[2\pi(-\alpha + 0.5)/N]| + |W[2\pi(-\alpha + 1.5)/N]|$ and $S = 2y_2 + y_1 = 2 \cdot |W[2\pi(-\alpha - 0.5)/N]| + |W[2\pi(-\alpha - 1.5)/N]|$, so the amplitude ratio is simplified as

$$\beta = \frac{R - S}{R + S} = f(\alpha) \quad (35)$$

According to the polynomial fitting, the frequency correction coefficient is obtained, as shown in (36):

$$\begin{aligned} \alpha = & 2.98440748 \cdot \beta + 0.55435577 \cdot \beta^3 \\ & + 0.24700564 \cdot \beta^5 + 0.14429796 \cdot \beta^7 + 0.10167482 \cdot \beta^9 \end{aligned} \quad (36)$$

The amplitude correction formula is

$$A = \frac{2(y_1 + 2y_2 + 2y_3 + y_4)}{R + S} \quad (37)$$

Let $g(\alpha) = (2 \cdot N / (R + S))$, according to the polynomial fitting, the amplitude correction coefficient is given as

$$\begin{aligned} g(\alpha) = & 1.46627405 + 0.22543298 \cdot \alpha^2 \\ & + 0.01855742 \cdot \alpha^4 + 0.00111283 \cdot \alpha^6 \end{aligned} \quad (38)$$

So, the amplitude correction formula of the FSLI algorithm is

$$A = (y_1 + 2y_2 + 2y_3 + y_4) \cdot g(\alpha) / N \quad (39)$$

The phase correction formula is

$$\theta = \arg [X(k_2 \cdot \Delta f)] - \pi \cdot \alpha \quad (40)$$

Also, the frequency correction formula is

$$f_0 = k_0 \cdot \Delta f = (k_2 - 0.5 + \alpha) \cdot f_s / N \quad (41)$$

3.5 Energy metering formula

The actual voltage and current signals are processed by the four kinds of windowed FFT interpolation formulas derived above; amplitude, phase and frequency of the fundamental and harmonic components of the voltage and the current signal under testing can be obtained accurately. Furthermore, the fundamental and harmonic energy can be calculated accurately.

For the orthogonality of the trigonometric function, it can be seen that there is no active energy between the different harmonic components of voltage and current. Therefore, the calculation formula of the fundamental and harmonic energy is simplified as follows:

$$W_n = \frac{1}{2} U_n I_n \cos(\alpha_n - \beta_n) k T \quad (42)$$

where W_n is the n th harmonic active energy, U_n and I_n are the amplitude of the n th harmonic voltage and the n th harmonic current, respectively. Parameters α_n and β_n are the initial phase of the n th harmonic voltage and the n th harmonic current, respectively. Parameter T is the fundamental period, and k is the number of the fundamental period. According to the IEC 61000-4-7 standard, it generally takes ten fundamental periods, that is, the time window length is about 200 ms.

The energy metering process including the fundamental harmonic, is as follows:

- (i) The FHSMW function is applied to the voltage and current signals, and then the FFT transform is carried out to obtain the spectrum of the voltage and current signals.
- (ii) Use the peak detection technology to detect the peak spectrum lines around the fundamental and harmonics of the voltage and current signals, respectively.
- (iii) Use one of the interpolation formula to calculate the amplitude ratio β around the fundamental and harmonics of the voltage and current signals, respectively.
- (iv) Use the value of β to calculate the frequency correction coefficient α .
- (v) Input α into the amplitude correction factor formula, the amplitude correction coefficient $g(\alpha)$ is calculated.
- (vi) Input α and $g(\alpha)$ into the amplitude, phase and frequency correction formula, then the amplitude, phase and frequency parameters of fundamental and harmonics of the voltage and current signals can be calculated accurately.
- (vii) Input the calculated parameters into the energy calculation formula, then the fundamental and harmonics energy is calculated precisely.

4 Simulation results

4.1 Simulation model

In order to verify the new harmonic analysis and energy metering algorithm, the mathematical model of the voltage and current signals with multiple harmonic components is selected, as shown in the following equation:

$$\begin{aligned} u(n) &= \sum_{k=1}^{13} U_k \sin(2\pi k f_0 n / f_s + \theta_{uk}) \\ i(n) &= \sum_{k=1}^{13} I_k \sin(2\pi k f_0 n / f_s + \theta_{ik}) \end{aligned} \quad (43)$$

where f_0 is the fundamental frequency, sampling rate $f_s = 4000$ Hz, and the components of the voltage and current model are listed in Table 1.

4.2 Algorithm simulation results with FHSMW

Based on the FHSMW function, four kinds of interpolation algorithms are applied to energy metering. The length of the window

Table 1 Components of the simulated harmonic signal

Harmonic order	U_k , V	θ_{uk} , °	I_k , A	θ_{ik} , °
1	220	32	10	29
2	3	20	0.15	5
3	15	68	0.8	64
4	2.5	46	0.13	77
5	10	19	0.65	49
6	2	85	0.10	15
7	8	53	0.48	61
8	2	28	0.05	37
9	3.5	50	0.32	53
10	1.5	16	0.03	20
11	2	72	0.21	38
12	1	40	0.05	25
13	1.5	10	0.15	20

Table 2 Simulation results with FHSMW

Order	Reference energy	Simulated results			
		SSLI	DSLII	TSLI	FSLI
1	219.6985	-1.2×10^{-4}	0.0	0.0	0.0
2	0.0435	2.1×10^{-1}	-1.7×10^{-4}	-5.0×10^{-6}	8.4×10^{-5}
3	1.1971	5.8×10^{-4}	2.0×10^{-6}	-1.0×10^{-6}	2.0×10^{-6}
4	0.0279	6.1×10^{-2}	-1.3×10^{-4}	-6.5×10^{-5}	7.4×10^{-5}
5	0.5629	5.9×10^{-3}	-1.1×10^{-5}	0.0	5.0×10^{-6}
6	0.0068	7.1×10^{-1}	-1.3×10^{-3}	7.7×10^{-4}	7.7×10^{-5}
7	0.3803	3.7×10^{-4}	2.0×10^{-6}	2.0×10^{-6}	3.0×10^{-6}
8	0.0099	8.3×10^{-2}	-2.2×10^{-4}	-2.1×10^{-4}	1.5×10^{-4}
9	0.1118	$6.3 \times 10^{-3} \times 10^{-3}$	-3.0×10^{-6}	4.0×10^{-6}	7.0×10^{-6}
10	0.0045	7.9×10^{-2}	-1.8×10^{-4}	-1.7×10^{-4}	1.6×10^{-4}
11	0.0348	1.0×10^{-2}	-3.5×10^{-5}	-6.1×10^{-5}	1.2×10^{-5}
12	0.0048	4.4×10^{-2}	-1.9×10^{-5}	1.7×10^{-4}	7.4×10^{-5}
13	0.0222	2.2×10^{-2}	-2.4×10^{-5}	1.0×10^{-5}	6.0×10^{-6}
total	222.1049	-1.5×10^{-5}	0.0	0.0	0.0

is 800 points, and the fundamental frequency is 50.1 Hz. The simulation results are given in Table 2.

The simulation results show that the more the spectrum lines in the algorithm, the higher the computing accuracy. That is, the FSLI algorithm has the highest computing accuracy and the SSLI algorithm has the lowest computing accuracy. The DSLI, TSLI and FSLI algorithms based on this new FHSMW can be proposed to harmonic analysis and energy metering.

4.3 Algorithm simulation results with different windows

The Hanning window, Blackman window, Blackman–Harris window and the new FHSMW are applied to the four-spectrum-line interpolation algorithm to calculate the energy metering. The length of the window function is also 800 points and the fundamental frequency is 50.1 Hz. The simulation results are given in Table 3.

The simulation shows that the accuracy of the energy metering algorithm based on the new FHSMW four-spectrum-line interpolation FFT has the highest computing accuracy compared with the other three algorithms, and the accuracy of the even harmonic energy is also greatly improved. The FHSMW function proposed in this paper has better amplitude–frequency characteristics.

4.4 Algorithm simulation results with fundamental frequency fluctuation

A large number of physical test results show that the power supply system fundamental frequency fluctuates in the range of 49.7–50.3 Hz. So, with the fundamental frequency fluctuation between 49.7 and 50.3 Hz, and a fluctuation interval of 0.1 Hz, the fundamental frequency fluctuation simulation was carried out based on the four-spectrum-line interpolation FFT algorithm with the Hanning window, Blackman window, Blackman–Harris window and FHSMW, to estimate the effects of the fundamental frequency fluctuation on the algorithm. The fundamental curve and the 5th harmonic curve are shown in Figs. 5 and 6, respectively.

It can be seen from Fig. 5 that the energy metering algorithm based on the Blackman–Harris window has the highest accuracy when the fundamental frequency is 49.9 Hz, but its calculation accuracy is influenced by the fundamental frequency fluctuation. However, the algorithm based on the new FHSMW has higher calculation accuracy of the fundamental energy, and the effect of the fundamental frequency fluctuation on this algorithm is the smallest. It can be seen from Fig. 6 that the accuracy of the 5th harmonic energy calculation based on the new FHSMW is higher than the other three algorithms as the fundamental frequency fluctuates. The new algorithm based on the new FHSMW is affected least by the fundamental frequency fluctuation.

Table 3 Simulation results with different windows

Order	Reference energy	Simulated results			
		Hanning	Blackman	Blackman–Harris	FHSMW
1	219.6985	-3.2×10^{-5}	-1.2×10^{-5}	0.0	0.0
2	0.0435	4.8×10^{-3}	3.2×10^{-3}	3.8×10^{-4}	8.4×10^{-5}
3	1.1971	-7.3×10^{-4}	-2.7×10^{-4}	0.0	2.0×10^{-6}
4	0.0279	5.9×10^{-3}	4.3×10^{-3}	-5.5×10^{-4}	7.4×10^{-5}
5	0.5629	-3.8×10^{-4}	1.9×10^{-5}	-2.8×10^{-4}	5.0×10^{-6}
6	0.0068	2.3×10^{-1}	1.1×10^{-1}	5.1×10^{-3}	7.7×10^{-5}
7	0.3803	-1.0×10^{-3}	-3.9×10^{-4}	-7.2×10^{-5}	3.0×10^{-6}
8	0.0099	-2.6×10^{-2}	-8.2×10^{-3}	-6.3×10^{-4}	1.5×10^{-4}
9	0.1118	-1.7×10^{-3}	-5.6×10^{-4}	-1.1×10^{-4}	7.0×10^{-6}
10	0.0045	-3.4×10^{-2}	-1.2×10^{-2}	-9.4×10^{-4}	1.6×10^{-4}
11	0.0348	2.7×10^{-3}	1.2×10^{-3}	-5.0×10^{-4}	1.2×10^{-5}
12	0.0048	-2.1×10^{-2}	-7.0×10^{-3}	-1.3×10^{-3}	7.4×10^{-5}
13	0.0222	3.1×10^{-3}	1.5×10^{-3}	-2.8×10^{-4}	6.0×10^{-6}
total	222.1049	-3.2×10^{-5}	-1.1×10^{-5}	-1.0×10^{-6}	0.0

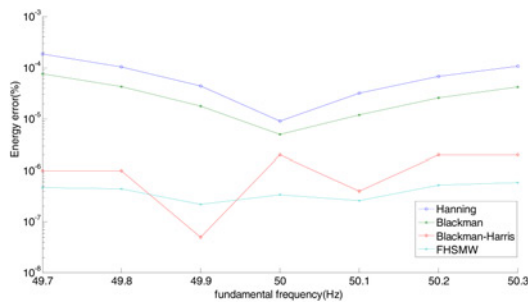


Fig. 5 Fundamental power relative errors under frequency fluctuation

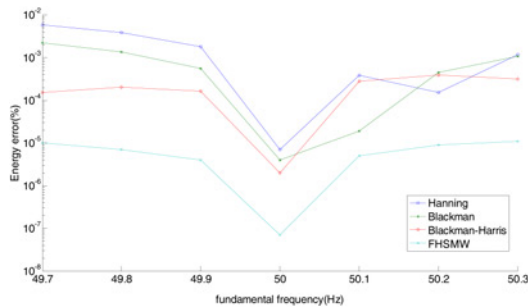


Fig. 6 Fifth-order harmonic power relative errors under frequency fluctuation

5 Conclusions

In this paper, a new FHSMW function is designed, and its time-domain expression and frequency-domain expression are also given. The analysis results show that it has better main-lobe and side-lobe performance. Based on the new FHSMW function, four kinds of harmonic analysis and energy metering algorithms, including SSLI, DSLI, TSLI and FSLI, are derived. The simulation results with four kinds of algorithm based on FHSMW show that the more the spectrum lines of the algorithm, the higher the computing accuracy. That is, the FSLI algorithm has the highest computing accuracy and the SSLI algorithm has the lowest computing accuracy. Compared with other three basic windows, the FSLI algorithm based on the new FHSMW has the highest computing accuracy and the accuracy of the even harmonic energy is also greatly improved, and the effect of the fundamental frequency fluctuation on the algorithm is minimal.

6 Acknowledgments

This paper is supported by the National High-Tech Research and Development Program of China (863 Program) under Grant no. 2015AA050404.

7 References

- [1] Davis E.J., Emanuel A.E., Pileggi D.J.: 'Harmonic pollution metering: theoretical considerations', *IEEE Trans. Power Del.*, 2000, **15**, (1), pp. 19–23
- [2] Belega D., Dallet D.: 'Frequency estimation via weighted multipoint interpolated DFT', *IET Sci., Meas. Technol.*, 2008, **2**, (1), pp. 1–8
- [3] Yang R., Xue H.: 'A novel algorithm for accurate frequency measurement using transformed consecutive points of DFT', *IEEE Trans. Power Syst.*, 2008, **23**, (3), pp. 1057–1062
- [4] Santamaria-Caballero I., Pantaleón-Prieto C.J., Ibanez-Diaz J., ET AL.: 'Improved procedures for estimating amplitudes and phases of harmonics with application to vibration analysis', *IEEE Trans. Instrum. Meas.*, 1998, **47**, (1), pp. 209–214
- [5] Agrež D.: 'Interpolation in the frequency domain to improve phase measurement', *Measurement*, 2008, **41**, (2), pp. 151–159
- [6] Liguori C., Paolillo A., Pignotti A.: 'Estimation of signal parameters in the frequency domain in the presence of harmonic interference: a comparative analysis', *IEEE Trans. Instrum. Meas.*, 2006, **55**, (2), pp. 562–569
- [7] Bracewell R.N., Bracewell R.N.: 'The Fourier transform and its applications' (McGraw-Hill, New York, 1986)
- [8] Grandke T.: 'Interpolation algorithms for discrete Fourier transforms of weighted signals', *IEEE Trans. Instrum. Meas.*, 1983, **32**, (2), pp. 350–355
- [9] Zhang F., Geng Z., Yuan W.: 'The algorithm of interpolating windowed FFT for harmonic analysis of electric power system', *IEEE Trans. Power Del.*, 2001, **16**, (2), pp. 160–164
- [10] Andria G., Savino M., Trotta A.: 'Windows and interpolation algorithms to improve electrical measurement accuracy', *IEEE Trans. Instrum. Meas.*, 1989, **38**, (4), pp. 856–863
- [11] Hidalgo R.M., Fernandez J.G., Rivera R.R., ET AL.: 'A simple adjustable window algorithm to improve FFT measurements', *IEEE Trans. Instrum. Meas.*, 2002, **51**, (1), pp. 31–36
- [12] Antoni J., Schoukens J.: 'A comprehensive study of the bias and variance of frequency-response-function measurements: optimal window selection and overlapping strategies', *Automatica*, 2007, **43**, (10), pp. 1723–1736
- [13] Testa A., Gallo D., Langella R.: 'On the processing of harmonics and interharmonics: using Hanning window in standard framework', *IEEE Trans. Power Del.*, 2004, **19**, (1), pp. 28–34
- [14] Zhou J., Wang X.-H., Qi C.-J.: 'Estimation of electrical harmonic parameters by using the interpolated FFT algorithm based on Blackman window', *J.-Zhejiang Univ.-Sci. Ed.*, 2006, **33**, (6), p. 650
- [15] Harris F.J.: 'On the use of windows for harmonic analysis with the discrete Fourier transform', *Proc. IEEE*, 1978, **66**, (1), pp. 51–83
- [16] Nuttall A.: 'Some windows with very good sidelobe behavior', *IEEE Trans. Acoust. Speech Signal Process.*, 1981, **29**, (1), pp. 84–91
- [17] Lin Y.-P., Vaidyanathan P.: 'A Kaiser window approach for the design of prototype filters of cosine modulated filterbanks', *IEEE Signal Process. Lett.*, 1998, **5**, (6), pp. 132–134
- [18] Wen H., Teng Z., Guo S., ET AL.: 'Hanning self-convolution window and its application to harmonic analysis', *Sci. China Ser. E: Technol. Sci.*, 2009, **52**, (2), pp. 467–476
- [19] Tianyuan T., Wenjuan C., Kaipei L., ET AL.: 'Harmonic analysis based on time domain mutual-multiplication window', *J. Mod. Power Syst. Clean Energy*, 2016, **4**, (1), pp. 47–53
- [20] Agrež D.: 'Weighted multipoint interpolated DFT to improve amplitude estimation of multifrequency signal', *IEEE Trans. Instrum. Meas.*, 2002, **51**, (2), pp. 287–292
- [21] Wu J., Zhao W.: 'A simple interpolation algorithm for measuring multi-frequency signal based on DFT', *Measurement*, 2009, **42**, (2), pp. 322–327